Bio-Medical Materials and Engineering 26 (2015) S665–S672
DOI 10.3233/BME-151358
IOS Press

Experiments and kinematics analysis of a hand rehabilitation exoskeleton with circuitous joints

Fuhai Zhang[a,b,*], Yili Fu[a,*], Qinchao Zhang[a] and Shuguo Wang[a]
[a]*State Key Laboratory of Robotics and System, Harbin Institute of Technology, Harbin 150001, China*
[b]*Postdoctoral Flow Station of Materials Science and Engineering, Harbin Institute of Technology, Harbin 150001, China*

Abstract. Aiming at the hand rehabilitation of stroke patients, a wearable hand exoskeleton with circuitous joint is proposed. The circuitous joint adopts the symmetric pinion and rack mechanism (SPRM) with the parallel mechanism. The exoskeleton finger is a serial mechanism composed of three closed-chain SPRM joints in series. The kinematic equations of the open chain of the finger and the closed chains of the SPRM joints were built to analyze the kinematics of the hand rehabilitation exoskeleton. The experimental setup of the hand rehabilitation exoskeleton was built and the continuous passive motion (CPM) rehabilitation experiment and the test of human-robot interaction force measurement were conducted. Experiment results show that the mechanical design of the hand rehabilitation robot is reasonable and that the kinematic analysis is correct, thus the exoskeleton can be used for the hand rehabilitation of stroke patients.

Keywords: Stroke patient, hand exoskeleton, continuous passive motion, circuitous joint

1. Introduction

Stroke, which often results in a combination of cognitive, sensory and motor impairments, has become one of the main diseases threatening human survival and health [1]. This disease reflects not only in upper and lower limbs but also in the loss of motor function of the hand [2]. It was verified by rehabilitation medicine that exercises with high strength and repeatability can stimulate cortical layer to recombine to help stroke patients learn to control the motion again [3]. Hand is one of the most important locomotive limbs of human, and the motor function of hand can be assisted by exoskeleton robots [4]. Many dexterous and advanced mechanisms of hand exoskeletons have been developed [5]. However, some of them are designed for master-slave systems [6] and some others are designed as force feedback device [7, 8].

[*] Address for correspondence: Fuhai Zhang, State Key Laboratory of Robotics and System, Harbin Institute of Technology, C1-302, No. 2 Yikuang Street, Harbin, Heilongjiang Province 150080, China. Tel.: +86-451-86403219; Fax: +86-451-86403219; E-mail: zfhhit@hit.edu.cn.
Yili Fu, State Key Laboratory of Robotics and System, Harbin Institute of Technology, Harbin 150001, China. Tel.: +86-451-86403219; Fax: +86-451-86403219; E-mail: meylfu@hit.edu.cn.

Recently, with the development of continuous passive motion (CPM), some rehabilitation robots based on CPM theory have been used widely in clinical training [9, 10]. The research conducted in [11] had developed the design of an EMG-driven exoskeleton robotic training device that can be employed for hand rehabilitation. Based on EMG signals, the system can understand the subject intention to move the hand, and the exoskeleton can assist the fingers' movement in order to perform some tasks [12]. However, they are limited in time delay and the number of independently actuated degrees of freedom (DOF). In other work, a wearable exoskeleton for hand rehabilitation of post-stroke has been developed that can perform the hand grasping and releasing [13]. The device employed a transmission mechanism of Bowden cable to perform the finger extension and flexion movement [14]. In the study conducted by Wege, et al. a hand exoskeleton has been studied where each finger has four degrees of freedom. Furthermore, this device can be easily attached and also be adjusted to different human hands [15]. Because, due to the special rehabilitation application, it is very important to make sure that exoskeleton and each finger joint have the same center of rotation, which avoids secondary injuries when the exoskeleton has close contact with the hand [16].

In this paper, we design and manufacture a novel hand exoskeleton. Our exoskeleton is designed specifically for the actual requirements of rehabilitation applications for stroke patients. We first developed a mechanical design of exoskeleton by employing a circuitous joint. Second, according to the characteristics of the closed chains of the SPRM joints, the kinematics of exoskeleton was analyzed. Lastly the CPM rehabilitation experiments and human-machine contact force test were conducted.

2. Description of a hand rehabilitation exoskeleton with circuitous joints

This hand exoskeleton is similar to a wearable glove, including three main parts, namely the adaptive dorsal finger exoskeleton, the adaptive dorsal metacarpal base and the Bowden cable driven actuator, as shown in Figure 1(a). The adaptive dorsal finger exoskeleton consists of five independent fingers, each of which has three joints and four rotational degrees of freedom (DOF), including a two-DOF metacarpophalangeal joint (MCP-1, MCP-2), a one-DOF proximal interphalangeal joint (PIP) and a one-DOF distal interphalangeal joint (DIP). In order to fit fingers of different thicknesses, the exoskeleton adopts a novel circuitous joint which can stretch and rotate at the same time, and the adjustable serial connection of three discrete joints makes the exoskeleton adjust to fingers of different lengths. The proposed circuitous joint employs the symmetrical pinion and rack mechanism (SPRM) with the parallel mechanism, as shown in Figure 1(b). The SPRM is designed to adapt to different fingers; the parallel sliding mechanism is adopted to avoid secondary injuries. So this exoskeleton can

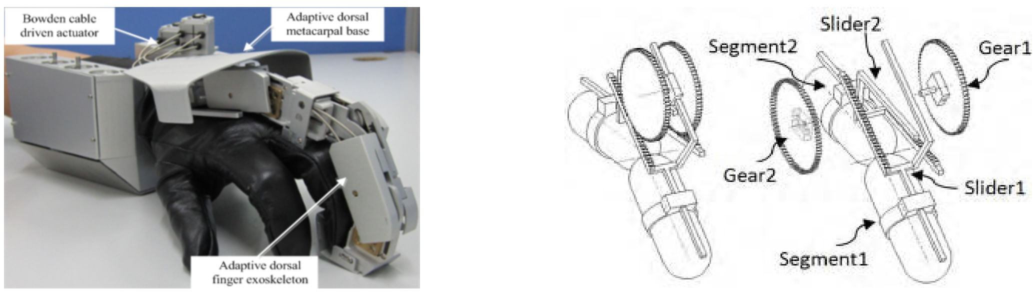

(a) (b)

Fig. 1. Hand rehabilitation exoskeleton: (a) overall structure. (b) SPRM with the parallel mechanism.

cover a wide workspace of a finger and adapt to a variety of fingers with different thicknesses [17].

3. Kinematics analysis

The exoskeleton finger is a serial mechanism composed of three closed-chain SPRM joints in series, which has the characteristics of both serial robots and parallel robots. Therefore, the finger exoskeleton can be treated as a serial robot made up of three joint exoskeleton parallel robots, and the kinematics analysis can be translated into the kinematics analysis issues of a finger open chain and three closed chains.

3.1. Kinematics analysis of finger's open chain

3.1.1. Forward kinematics

According to the design ideas of the project, the DOF configuration of the thumb is the same with that of the other fingers, so we can take any one of the fingers as the analysis object. Take the middle finger as an example, shown in Figure 2(a). The middle finger has four DOF, which can be treated as a manipulator with four rotational joints. The axis A_1 of joint MCP-1 is vertical. The axis A_2 of joint MCP-2 is perpendicular to A_1, and the axis A_3 of joint PIP is parallel to A_2. The axis A_4 of joint DIP is parallel to A_3. The coordinates of the links are shown in Figure 2(b). The base coordinate is fixed to the palm, and the origin O_0 is set to the intersection of axis A_1 and axis A_2.

In the coordinates established above, the link D-H parameters and the joint variables of the main kinematic chain are shown in Table 1.

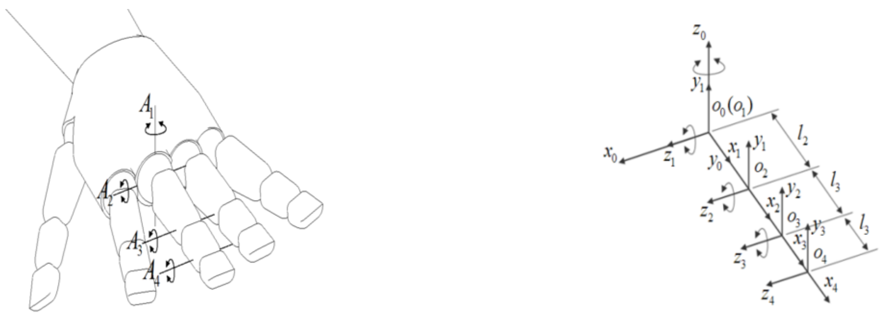

(a) (b)

Fig. 2. The coordinate establishing method of the middle finger: (a) The DOF analysis of the middle finger. (b) The coordinates of the links of the middle finger.

Table 1

The link parameters and the joint variables of the main open chain

joint i	θ_i (°)	d_i	a_i	α_i (°)	variation range(°)
1	θ_1	0	0	90	85-95
2	θ_2	0	l_2	0	0-90
3	θ_3	0	l_3	0	0-95
4	θ_4	0	l_4	0	0-70

According to the Denavit-Hartenberg (D-H) parametric modeling method, the homogeneous transformation matrix describing the relation between coordinates can be written as

$$ {}^{i-1}\boldsymbol{T}_i = \begin{bmatrix} \cos\theta_i & -\sin\theta_i\cos\alpha_i & \sin\theta_i\sin\alpha_i & a_i\cos\theta_i \\ \sin\theta_i & \cos\theta_i\cos\alpha_i & -\cos\theta_i\sin\alpha_i & a_i\sin\theta_i \\ 0 & \sin\alpha_i & \cos\alpha_i & d_i \\ 0 & 0 & 0 & 1 \end{bmatrix}. \tag{1} $$

According to Table 1 and Eq. (1), we can have the homogeneous transformation matrices of the adjacent links, $\boldsymbol{T}_1, \boldsymbol{T}_2, \boldsymbol{T}_3, \boldsymbol{T}_4$. The homogeneous transformation matrix of the end-effector of the main kinematic chain of the hand rehabilitation exoskeleton (i.e. the distal phalanx) relative to the base coordinate can be obtained and simplified as follows

$$ {}^{0}\boldsymbol{T}_4 = \boldsymbol{T}_1\boldsymbol{T}_2\boldsymbol{T}_3\boldsymbol{T}_4 = \begin{bmatrix} c_1c_{234} & -c_1s_{234} & s_1 & c_1(l_2c_2+l_3c_{23}+l_4c_{234}) \\ s_1c_{234} & -s_1s_{234} & -c_1 & s_1(l_2c_2+l_3c_{23}+l_4c_{234}) \\ s_{234} & c_{234} & 0 & l_2\mathrm{s}_2+l_3\mathrm{s}_{23}+l_4\mathrm{s}_{234} \\ 0 & 0 & 0 & 1 \end{bmatrix} = \begin{bmatrix} \boldsymbol{n} & \boldsymbol{o} & \boldsymbol{a} & \boldsymbol{p} \\ 0 & 0 & 0 & 1 \end{bmatrix} = \begin{bmatrix} n_x & o_x & a_x & p_x \\ n_y & o_y & a_y & p_y \\ n_z & o_z & a_z & p_z \\ 0 & 0 & 0 & 1 \end{bmatrix}, \tag{2} $$

where s_{234} represents $\sin(\theta_2+\theta_3+\theta_4)$, c_{234} represents $\cos(\theta_2+\theta_3+\theta_4)$, s_{23} represents $\sin(\theta_2+\theta_3)$, c_{23} represents $\cos(\theta_2+\theta_3)$, s_1 represents $\sin\theta_1$, c_1 represents $\cos\theta_1$, s_2 represents $\sin\theta_2$, c_2 represents $\cos\theta_2$, $[\boldsymbol{n}\ \ \boldsymbol{o}\ \ \boldsymbol{p}]_{3\times 3}$ represents the attitude matrix of the end-effector, $\boldsymbol{p}_{3\times 1}$ represents the position vector of the end-effector.

3.1.2. Inverse kinematics

From Eq. (2), and take the actual value ranges of θ_1, θ_2, θ_3 and θ_4 into consideration, we have

$$ \begin{cases} \theta_1 = \arctan(p_y/p_x) + k\pi, \\ \theta_2 = \arcsin(B/\sqrt{C^2+D^2}) - \arctan(D/C) + k\pi, \\ \theta_3 = \arccos((A^2+B^2-l_2^2-l_3^2)/(2l_2l_3)) + k\pi, \\ \theta_4 = \arctan n_x/o_x - \theta_3 - \theta_2 + k\pi, \end{cases} \tag{3} $$

where $A = p_y/a_x - l_4o_z$, $B = p_z - l_4n_z$, $C = l_2 + l_3\cos\theta_3$, $D = l_3\sin\theta_3$.

3.2. Kinematics analysis of exoskeleton closed chain

3.2.1. One-DOF SPRM with the parallel mechanism

The joints PIP and DIP of the finger's open chain belong respectively to two one-DOF closed chain mechanisms. The two joints' structures are the same, so the two one-DOF closed chain mechanisms also have the same structure which is made up of a one-DOF SPRM with the parallel mechanism and two adjacent segments. The structure and the definitions of relevant parameters are shown in Figure 3(a).

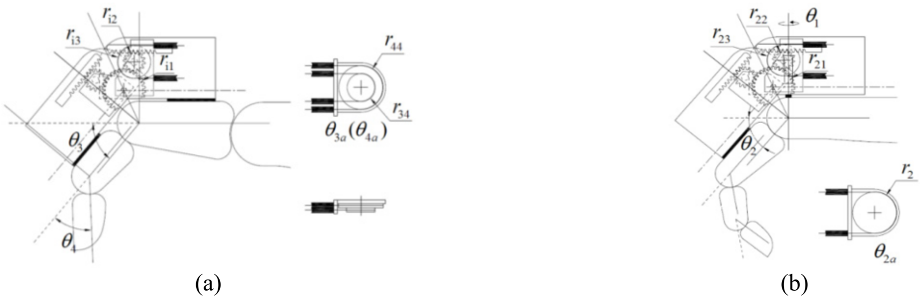

Fig. 3. Structure of joints: (a). One-DOF SPRM with parallel mechanism. (b). Two-DOF SPRM with parallel mechanism.

From the structural features of the SPRM with the parallel mechanism, we can get the structural equation of the closed chain

$$\theta_{ia} = \frac{r_{i1}}{r_{i2}} \cdot \frac{r_{i3}}{r_{i4}} \cdot \theta_i \ , \tag{4}$$

where r_{i1} r_{i2} represent the radiuses of gears; r_{i3} , r_{i4} represent the radiuses of wire wheels; θ_{ia} represents the rotational angle of motor, $i = 3,4$.

The joints PIP and DIP of the exoskeleton are driven in coupled pattern, and the coupling ratio is adjusted by changing the radius of the wire wheels connected to the motor shaft. Therefore, the structural equation of the coupled closed-chain mechanism of joints PIP and DIP can be written as

$$\begin{bmatrix} \theta_{3a} \\ \theta_{4a} \end{bmatrix} = \begin{bmatrix} r_{31}/r_{32} \cdot r_{33}/r_{34} & 0 \\ 0 & r_{41}/r_{42} \cdot r_{43}/r_{44} \end{bmatrix} \cdot \begin{bmatrix} \theta_3 \\ \theta_4 \end{bmatrix}. \tag{5}$$

3.2.2. Two-DOF SPRM with the parallel mechanism

The joints MCP-1 and MCP-2 of the finger main open chain are two rotational joints with intersecting axes that can be treated as a hooke joint (joint MCP) with two rotational DOF. In the overall exoskeleton system, joint MCP and a two-DOF SPRM with the parallel mechanism together constitute a closed chain whose structure is shown in Figure 3(b). The structural equation of the SPRM with the parallel mechanism is the same with that of joints PIP and DIP. As the rotation range of joint MCP-1 is small, the joint is a passive joint that is not driven. Thus, the structural equation of the two-DOF SPRM with the parallel mechanism can be written as

$$\begin{bmatrix} \theta_{1a} \\ \theta_{2a} \end{bmatrix} = \begin{bmatrix} 1 & 0 \\ 0 & r_{21}/r_{22} \cdot r_{23}/r_{24} \end{bmatrix} \cdot \begin{bmatrix} \theta_1 \\ \theta_2 \end{bmatrix}. \tag{6}$$

4. CPM experiments of hand rehabilitation exoskeleton

The CPM rehabilitation experiment process is shown in Figures 4-6. In order to test the adaptability of joint PIP and joint DIP of the exoskeleton robot to fingers of different sizes and considering that the joint PIP and DIP of the human hand are always coupled in the daily life, the CPM rehabilitation

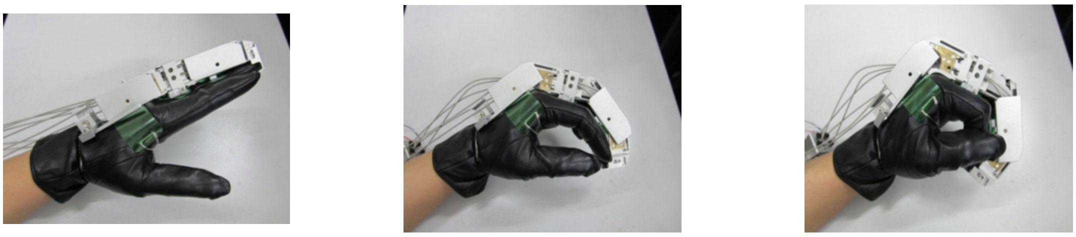

(a) (b) (c)

Fig. 4. CPM rehabilitation experiment of joints PIP and DIP of middle finger.

(a) (b) (c)

Fig. 5. CPM rehabilitation experiment of joints PIP and DIP of ring finger.

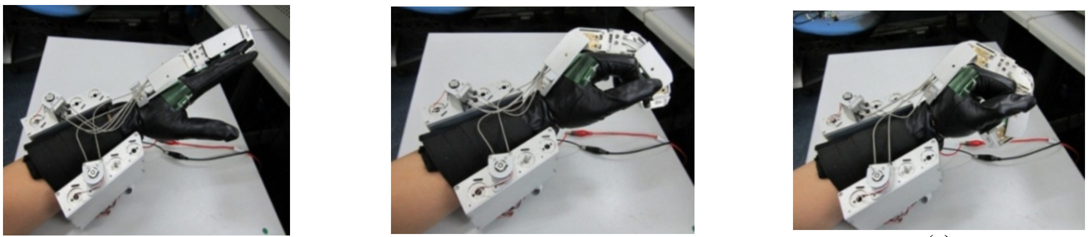

(a) (b) (c)

Fig. 6. CPM rehabilitation experiment of the finger.

training is conducted simultaneously on the joint PIP and DIP of the middle finger and the ring finger, as shown in Figures 4 and 5, respectively. The CPM rehabilitation training of three joints can simulate the grabbing and fisting motions through controlling the speed of the motors in order to achieve the function rehabilitation of the patients. The CPM rehabilitation experiments of three joints are shown in Figure 6.

In order to verify the feasibility of the human interaction of the hand rehabilitation exoskeleton, relevant experiment was done on it, as shown in Figure 7. First, force sensors Flexiforce were installed on the mechanism of the finger exoskeleton according to the design requirements and the resistances of the sensors were measured to ensure the functioning. Then, the driving mechanism of the finger exoskeleton was worn on the middle finger and the force sensors were adjusted properly. Last, connect the sensors and the conditioning circuit that was connected to the computer through the Data Acquisition Card MPS-010501 and the data was gathered during the experiment. The independent intermittent flexion of joint MCP-2, the coupling intermittent flexion of joints PIP and DIP and the intermittent flexion of the whole finger are done and the signals gathered by the sensors are shown in Figure 8. Four pressure sensors are installed on the single finger of the exoskeleton robot. In Figure 8, plot 0 is the pressure on the palmar side of DIP, plot 1 is the pressure on the dorsal side of DIP, plot 2 is the pressure on the dorsal side of MCP-2, and plot 3 is the pressure on the dorsal side of PIP.

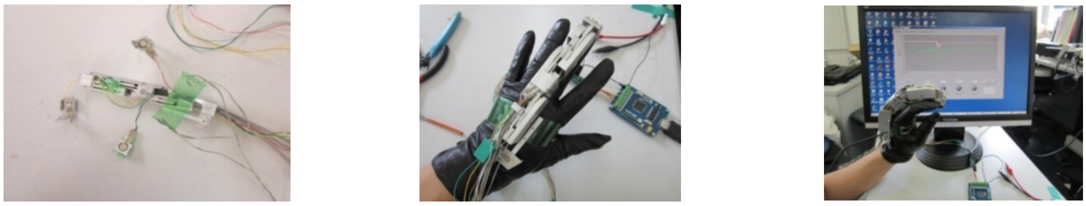

(a) (b) (c)

Fig. 7. The human interaction determination experiment: (a) The installation of the force sensors. (b) The adjustment of the force sensors. (c) Experiment and data gathering.

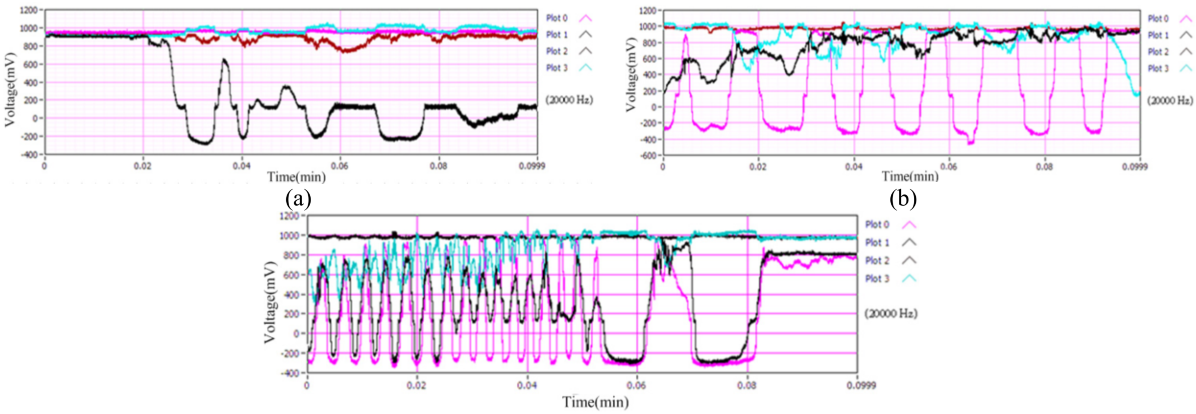

(a) (b) (c)

Fig. 8. The signals of the force sensors during typical motions: (a) The independent slow bending of joint MCP-2. (b) The coupling intermittent bending of joints PIP and DIP. (c) The intermittent natural bending of the finger.

5. Discussion and conclusion

The adaptability to hands of different sizes is an important criterion to evaluate the design of the hand rehabilitation exoskeleton. Compared with other research outcomes, the exoskeleton we designed can adapt to the thickness changes of the finger joints. The experiment results in Figures 4 and 5 are 2-DOF finger adaptability experiments. The results show that the same finger exoskeleton can be worn tightly on both the middle finger and the ring finger, whose lengths and thicknesses are different, and in both conditions, the finger can move flexibly and the joints will not be stretched or squeezed. The experiment results in Figure 6 show that the adjustable connection of the three joints can make the robot adapt to the length changes of the finger phalanxes, and the joints have good adaptability. The human-robot interaction force experiments were conducted in Figure 7. Experiment results shown in Figure 8 show that the verifying scheme of the human interaction of the hand rehabilitation exoskeleton is rational and that the signals gathered by the force sensors can reflect the endeavor of the patients.

Therefore, experiment results show that the mechanical design of the hand rehabilitation robot is rational, thus the exoskeleton can be used for hand rehabilitation of stroke patients. In addition, according to the characteristics of the closed chains of the SPRM joints, the kinematic equations of the open chain of finger and the closed chains of SPRM joints were built to analyze the kinematic issues of the hand rehabilitation robot.

Acknowledgments

This work is supported in part by the National Natural Science Foundation of China (Grant No. 61203347), Self-Planned Task (No. SKLRS201501C) of State Key Laboratory of Robotics and System (HIT), the Fundamental Research Funds for the Central Universities (Grant No. HIT. NSRIF. 2013047) and China Postdoctoral Science Foundation (Grant No. 2013M531023).

References

[1] P.M. Kelly-Hayes, J.T. Robertson, J.P. Broderick, et al., The American heart association stroke outcome classification, Stroke **29** (1998), 1274–1280.
[2] V.L. Feigin, Stroke epidemiology in the developing world, The Lancet **365** (2005), 2160–2161.
[3] B. French, L.H. Thomas, M.J. Leathley, et al., Repetitive task training for improving functional ability after stroke, Stroke **40** (2009), e98–e99.
[4] H.I. Krebs, N. Hogan, M.L. Aisen, et al., Robot-aided neurorehabilitation, IEEE Transactions on Rehabilitation Engineering **6** (1998), 75–87.
[5] T.T. Worsnopp, M.A. Peshkin, J.E. Colgate, et al., An actuated finger exoskeleton for hand rehabilitation following stroke, Proceedings of the IEEE International Conference on Rehabilitation Robotics, Noordwijk, Netherlands, 2007, pp. 896–901.
[6] H. Fang, Z. Xie and H. Liu, An exoskeleton master hand for controlling DLR/HIT hand, Proceedings of the IEEE/RSJ International Conference on Intelligent Robots and Systems, St. Louis, USA, 2009, pp. 3703–3708.
[7] S. Nakagawara, H. Kajimoto, N. Kawakami, et al., An encounter-type multi-fingered master hand using circuitous joints, Proceedings of the IEEE International Conference on Robotics and Automation, Barcelona, Spain, 2005, pp. 2667–2672.
[8] M. Bouzit, G. Burdea, G. Popescu, et al., The rutgers master II-new design force-feedback glove, IEEE/ASME Transactions on Mechatronics **7** (2002), 256–263.
[9] Y. Fu, P. Wang, S. Wang, et al., Design and development of a portable exoskeleton based CPM machine for rehabilitation of hand injuries, Proceedings of the IEEE International Conference on Robotics and Biomimetics, Sanya, China, 2007, pp. 1476–1481.
[10] S. Ueki, H. Kawasaki, S. Ito, et al., Development of a hand-assist robot with multi-degrees-of-freedom for rehabilitation therapy, IEEE/ASME Transactions on Mechatronics **17** (2012), 136–146.
[11] N.S.K. Ho, K.Y. Tong, X.L. Hu, et al., An EMG-driven exoskeleton hand robotic training device on chronic stroke subjects: Task training system for stroke rehabilitation, Proceedings of the IEEE International Conference on Rehabilitation Robotics, Zurich, Switzerland, 2011, pp. 1–5.
[12] M. Mulas, M. Folgheraiter and G. Gini, An EMG-controlled exoskeleton for hand rehabilitation, Proceedings of the IEEE International Conference on Rehabilitation Robotics, Chicago, USA, 2005, pp. 371-374.
[13] M. Cempini, S.M.M. De Rossi, T. Lenzi, et al., Kinematics and design of a portable and wearable exoskeleton for hand rehabilitation, Proceedings of the IEEE International Conference on Rehabilitation Robotics, Seattle, USA, 2013, pp. 1–6.
[14] M.A. Rahman and A. Al-Jumaily, Design and development of a hand exoskeleton for rehabilitation following stroke, Procedia Engineering **41** (2012), 1028–1034.
[15] A. Wege and G. Hommel, Development and control of a hand exoskeleton for rehabilitation of hand injuries, Proceedings of the IEEE/RSJ International Conference on Intelligent Robots and Systems, Edmonton, Canada, 2005, pp. 3046–3051.
[16] P. Heo, G.M. Gu, S. Lee, et al., Current hand exoskeleton technologies for rehabilitation and assistive engineering, International Journal of Precision Engineering and Manufacturing **13** (2012), 807–824.
[17] F. Zhang, L. Hua, Y. Fu, et al., Design and development of a hand exoskeleton for rehabilitation of hand injuries, Mechanism and Machine Theory **73** (2014), 103–116.